Low-thrust trajectory optimization of asteroid sample return mission with multiple revolutions and moon gravity assists

TANG Gao, JIANG FangHua* & LI JunFeng

School of Aerospace Engineering, Tsinghua University, Beijing 100084, China

Near-Earth asteroids have gained a lot of interest and the development in low-thrust propulsion technology makes complex deep space exploration missions possible. A mission from low-Earth orbit using low-thrust electric propulsion system to rendezvous with near-Earth asteroid and bring sample back is investigated. By dividing the mission into five segments, the complex mission is solved separately. Then different methods are used to find optimal trajectories for every segment. Multiple revolutions around the Earth and multiple Moon gravity assists are used to decrease the fuel consumption to escape from the Earth. To avoid possible numerical difficulty of indirect methods, a direct method to parameterize the switching moment and direction of thrust vector is proposed. To maximize the mass of sample, optimal control theory and homotopic approach are applied to find the optimal trajectory. Direct methods of finding proper time to brake the spacecraft using Moon gravity assist are also proposed. Practical techniques including both direct and indirect methods are investigated to optimize trajectories for different segments and they can be easily extended to other missions and more precise dynamic model.

sample return, optimization, gravity assist

PACS number(s): 02.60.Pn, 05.45.Ca, 45.80.+r

1 Introduction

Small bodies in the Solar System have gained a great deal of attention for several decades. Investigation of them can not only help to discover the formation of the Solar System, but also for economical purposes [1]. Compared with small objects in other regions, near-Earth asteroid (NEA) exploration is a relatively easy mission because less fuel and period are needed to rendezvous with the selected target. They are also the nearest threat to the Earth, the most hopeful candidates to be captured [2] and best destination for sampling.

The problem of the 6th Competition of Trajectory Optimization of China (CTOC) is a low-Earth Orbit (LEO) to NEA sample return mission. The spacecraft has to start from

a LEO to rendezvous with an asteroid and bring maximum mass of sample back to near-Earth region. The possibility of using current technology to bring sampling or even capture NEA have already been discussed. NASA has proposed the Asteroid Redirection Mission (ARM) aiming to capture a NEA to an stable orbit around the Moon [3]. Methods to capture NEAs to near-Earth region in the Sun-Earth restricted three-body problem model have been investigated in literature [4,5].

1.1 Low-thrust trajectory optimization

Compared with traditional high-thrust chemical propulsion, low-thrust electric propulsion has much higher specific impulse and it's suited for long-time deep-space mission. Due to its higher specific impulse, electric propulsion is more effi-

*Corresponding author (email: jiangfh@tsinghua.edu.cn)

cient. The launch of NASA's Deep Space I [6] demonstrated the first use of ion propulsion in interplanetary mission. And later missions such as SMART-I [7], Hayabusa [8], DAWN [9] also take advantage of low-thrust propulsion to increase the payload mass and reduce the fuel cost. Long thrusting time is necessary to get enough velocity increment as the thrust is very low. Because of the continuous and durable low thrust, it's rather difficult to find the optimal trajectory for a mission with low-thrust electric propulsion. Lots of research has been conducted to design the optimal low-thrust trajectory.

Methods for optimizing low-thrust trajectories are typically categorized as direct methods [10–12] and indirect methods [13–16], the combinations of which are termed hybrid methods [17,18]. Direct methods convert optimal control problem into a nonlinear programming problem (NLP) through parameterization. Usually numerous variables are needed, which increase the amount of computational effort. Indirect methods take effort of calculus of variation and convert the optimal control problem into a two-point boundary value problem (TPBVP). The variables to be solved are initial costate variables and they are hard to guess because of their lack of physical meanings. The solution to the TPBVP is very difficult to obtain because of the narrow convergence domain. Hybrid methods combine the advantage of both direct and indirect methods. The thrust structure is usually presupposed, and the optimal control is determined by the optimality condition of indirect methods. Instead of building a TPBVP, the problem is transformed into a NLP.

Hull [19] summarized four types of direct methods on interplanetary low-thrust trajectory optimization. Typical direct methods include collocation methods [10], differential inclusion [20], Gauss pseudo-spectral method [21] and genetic algorithms [22,23].

The Pontryagins minimum principle (PMP) indicates that, the fuel-optimal control is bang-bang control. It's difficult to solve such problem if the switching rules are not given in advance, due to narrow convergence domain, discontinuous integrated functions and singularity of Jacobian matrix [16,24]. To overcome the difficulty, methods such as assigning the switching structure a priori [24,25], using fuel consuming model which leads to continuous control [26], and reducing the dimension of the problem [27] are proposed. These methods are inefficient and have the possibility of missing the optimal solution if the wrong switching structure is assigned. Recently, the homotopic approaches have been applied to solve bang-bang control problems [15,16,28,29]. The principle of a homotopic approach is to solve a difficult problem by starting from the solution of a related but easier problem. A perturbation of energy form is added to the performance index, which leads to continuous control and larger convergence domain. By gradually reducing the energy form and taking the obtained solution as an initial guess for next iteration, fuel-optimal control can be approached.

Generally speaking, direct methods have a larger conver-

gence domain and it's very convenient to impose constraints such as gravity assist when direct methods are used. The initial guess is also easier to give according to its physical meaning. Although the precision of some methods are worse than indirect methods and the results of direct methods are often suboptimal. Indirect methods are more likely to result in a global optimum if a good initial guess is given and the convergence process is very quick. Hybrid methods have both the advantages and disadvantages of direct and indirect methods. In this paper, both direct and indirect methods with homotopic approaches are investigated according to their own practical properties.

1.2 Gravity assist

Gravity assist is essential to deep-space mission design because proper use of gravity assists can significantly reduce the fuel consumption and thus increase the mass of paylaod. For a mission which is started from LEO and only low-thrust electric propulsion can be used to escape the Earth, Moon gravity assists are often used to reduce the fuel consumption and increase the escaping velocity. Moon gravity assist have been widely used in mission design [30,31]. For spacecrafts departing the Earth-Moon system, Moon gravity assists can significantly increase the hyperbolic escape energy ($C_3 = v^2 - 2\mu_{\text{Earth}}/r$ in km^2/s^2) with an acceptable time increment. Although the increment in C_3 may vary in different cases, two gravity assists with the help of resonant orbits always have a much higher C_3 increment than a single gravity assist if properly designed.

Not only for escaping, Moon gravity assist can also be used to brake the spacecraft for capturing [32]. The design of Moon gravity assist strategies both in simple and precise dynamic model are proposed in this paper.

Gravity assist is often modeled as an instant impulse [33] in preliminary design. That is to say, the time for the spacecraft to enter and leave the gravity assist celestial body is neglected and the position before and after gravity assist is the same with that of the gravity assist celestial body and the relative speed, which is called hyperbolic escape speed, note as v_∞, turns an angle which is determined by the magnitude of relative speed, minimum flyby altitude and gravitational parameter of the celestial body. The magnitude of hyperbolic escape speed stays the same after gravity assist, while the turn angle θ is relative to gravity assist radius r_p and escape speed v_∞, with the relation

$$\sin \frac{\theta}{2} = \frac{1}{1 + v_\infty^2 r_p / \mu_a}. \qquad (1)$$

After gravity assist, the spacecraft may be guided into a resonant orbit whose period with the gravity assist celestial body is a ratio of integers, note as $m : n$. In this situation, another opportunity of gravity assist occurs after m revolutions of the celestial body. This procedure can be continued until

a certain terminal condition is satisfied. Multiple gravity assists can change the energy of the spacecraft gradually and no other maneuvers are needed with the help of resonant orbits.

2 Problem statement

The background of the 6th CTOC is asteroid sample return mission. The launch window is from Modified Julian Dates (MJD) 59215 (January 1, 2021) to MJD 62867 (December 31, 2030). The spacecraft starts from a circular LEO with the altitude of 200 km and arbitrary inclination between 20° and 90°. Then after escaping from the Earth it should rendezvous with an asteroid that belongs to the 792 candidates specified by the organizer. After staying for at least 30 d, it should bring maximum sample back to the Earth from the asteroid. The final state is considered feasible if it satisfies

$$r_{\text{sc}} = 6578 \text{ km}, v_{\text{sc}} \leqslant 11 \text{ km/s}, \tag{2}$$

where r_{sc} is the spacecraft's distance from the Earth, v_{sc} the relative speed, and the mission time is 10 years at most. And for the convenience of computing, the direction of the coordinates of Earth Central Inertial Frame (ECI) is manually chosen to be the same with that of Heliocentric Ecliptic Inertial Reference Frame (HEIRF).

The gravity of Earth, Moon and Sun are all considered in the entire mission and the gravity of asteroid is neglected. The distance from the spacecraft to the Moon should not be less than 1838 km. And the motion of the Sun and Moon relative to the Earth, the asteroid relative to the Sun are all considered in two-body model. The dynamic function of the spacecraft in ECI is given by the organizer

$$\ddot{\boldsymbol{r}} = -\frac{\mu_{\text{E}}}{r^3}\boldsymbol{r} - \mu_{\text{M}}\left(\frac{\boldsymbol{r}_{\text{M}}}{r_{\text{M}}^3} + \frac{\boldsymbol{r} - \boldsymbol{r}_{\text{M}}}{\|\boldsymbol{r} - \boldsymbol{r}_{\text{M}}\|^3}\right)$$
$$- \mu_{\text{S}}\left(\frac{\boldsymbol{r}_{\text{S}}}{r_{\text{S}}^3} + \frac{\boldsymbol{r} - \boldsymbol{r}_{\text{S}}}{\|\boldsymbol{r} - \boldsymbol{r}_{\text{S}}\|^3}\right) + \frac{\boldsymbol{T}}{m_{\text{sc}}},$$
$$0 \leqslant T = \sqrt{(T_x^2 + T_y^2 + T_z^2)} = 10 \text{ N}, \tag{3}$$
$$\dot{m}_{\text{sc}} = -\frac{T}{I_{\text{sp}}g_0},$$

where $\mu_{\text{E}}, \mu_{\text{M}}, \mu_{\text{S}}$ are the gravitational constant of the Earth, Moon and Sun, $\boldsymbol{r}, \boldsymbol{r}_{\text{M}}, \boldsymbol{r}_{\text{S}}$ the position vector from the Earth to the spacecraft, Moon and Sun, I_{sp} the specific impulse, g_0 the gravitational acceleration at sea level, m_{sc} the mass of the spacecraft, $\boldsymbol{T}$ the thrust vector and T its magnitude. This dynamic function is correct on condition that both the gravity of the Sun and Moon are considered for the motion of the Earth, which is in conflict with the presupposed two-body model, although the difference is rather small. Because the data check program provided by the organizer is based on this dynamic model, the dynamic function of the spacecraft in HEIRF is derived by substituting $\boldsymbol{r}_{\text{E}x} = \boldsymbol{r}_{\text{S}x} - \boldsymbol{r}_{\text{SE}}$, where x donates the four bodies in this problem, into eq. (3). The dynamic function in HEIRF is obtained

$$\ddot{\boldsymbol{r}} = \ddot{\boldsymbol{r}}_{\text{SE}} + \ddot{\boldsymbol{r}}_{\text{EC}}$$

$$= \ddot{\boldsymbol{r}}_{\text{SE}} - \frac{\mu_E}{r_{\text{EC}}^3}\boldsymbol{r}_{\text{EC}} - \mu_{\text{M}}\left(\frac{\boldsymbol{r}_{\text{EM}}}{r_{\text{EM}}^3} + \frac{\boldsymbol{r}_{\text{EC}} - \boldsymbol{r}_{\text{EM}}}{\|\boldsymbol{r}_{\text{EC}} - \boldsymbol{r}_{\text{EM}}\|^3}\right)$$
$$- \mu_{\text{S}}\left(\frac{\boldsymbol{r}_{\text{ES}}}{r_{\text{ES}}^3} + \frac{\boldsymbol{r}_{\text{EC}} - \boldsymbol{r}_{\text{ES}}}{\|\boldsymbol{r}_{\text{EC}} - \boldsymbol{r}_{\text{ES}}\|^3}\right) + \frac{\boldsymbol{T}}{m_{\text{sc}}}$$
$$= \frac{\boldsymbol{T}}{m_{\text{sc}}} - \mu_{\text{S}}\frac{\boldsymbol{r}_{\text{SC}}}{r_{\text{SC}}^3} - \mu_{\text{E}}\frac{\boldsymbol{r}_{\text{SC}} - \boldsymbol{r}_{\text{SE}}}{\|\boldsymbol{r}_{\text{SC}} - \boldsymbol{r}_{\text{SE}}\|^3}$$
$$- \mu_{\text{M}}\left(\frac{\boldsymbol{r}_{\text{EM}}}{r_{\text{EM}}^3} + \frac{\boldsymbol{r}_{\text{SC}} - \boldsymbol{r}_{\text{SE}} - \boldsymbol{r}_{\text{EM}}}{\|\boldsymbol{r}_{\text{SC}} - \boldsymbol{r}_{\text{SE}} - \boldsymbol{r}_{\text{EM}}\|^3}\right), \tag{4}$$

where $\boldsymbol{r}_{xy}$ denotes the position vector from body x to body y and S, E, M, C denotes the Sun, Earth, Moon, spacecraft.

As for the parameters of low-thrust propulsion, its specific impulse is 3000 s and the maximum thrust magnitude is 10 N. The initial mass of the spacecraft is 2000 kg of which 1500 kg is fuel. The performance index of the mission is to maximize the mass of sample from the asteroid.

$$\text{Maximize}: \ J = m_{\text{sample}}. \tag{5}$$

In the problem statement above, some techniques are beyond current aerospace techniques and are promising to be implemented in the near future. Some parameters such as the magnitude of thrust seems unrealistic. However, it doesn't matter to investigate this problem for possible mission design in the future.

3 Problem analysis

Although some techniques have been proposed to reduce the difficulty of low-thrust trajectory optimization problem when indirect methods are used [15,16], a mission with many revolutions and multiple gravity assists is still hard to design and optimize if only indirect methods are used, as the large number of revolutions and the long mission time significantly increase the sensitivity of the problem. For complex missions, different methods are required for different segments. And in this paper both direct and indirect methods are used to solve different problems in different segments of the mission that we are investigating.

To escape from the Earth starting from LEO only using low-thrust propulsion, a good way is to raise the altitude of apogee gradually without greatly raising the altitude of perigee at the same time, which is similar to traditional Hohmann transfers and this strategy results in a high-eccentricity orbit. The engine is turned on only when the spacecraft is near its perigee and because of the low thrust we can only get finite velocity increment for every revolution so large number of revolutions are required. As the apogee increase slowly, total mission time is long. The gravity of the Moon and the Sun have significant influence on the motion of the spacecraft, which aggravates the sensitivity of equations of motion. When the sensitivity increases, trajectory optimization becomes more difficult to solve.

Because the number of revolutions is large and the mission time is long, numerical integration is inefficient. To speed up

the calculation of the problem, a parallel computing method which is easy to accomplish is used. A multiple shooting method is proposed to decrease the sensitivity of the problem, which is especially suited for parallel computing.

After escaping from and before reentering the Earth-Moon system, the problem is considered with the Sun as the dominating gravity source, and indirect methods are used to optimize the trajectory to maximize the mass collected. Homotopic methods are applied to overcome the difficulty of bang-bang control.

To simplify the problem, the mission is divided into 5 steps.

(1) LEO Escape. From LEO, apply thrust when the spacecraft is near its perigee to raise the altitude of apogee gradually until the spacecraft is able to coast into the Moon's sphere of influence (SOI).

(2) Moon Gravity Assist. Use two Moon gravity assists to help the spacecraft to reach the velocity to be able to escape from the Earth's SOI.

(3) Fly to Asteroid. The spacecraft flies to the target asteroid with low-thrust propulsion.

(4) Fly Back to the Earth. After sampling, the spacecraft flies back to Earth's SOI.

(5) Capture. Brake the spacecraft with the help of Moon gravity assist to meet the final condition.

The mission is divided into 5 steps because of the complexity of the problem. It is almost impossible to optimize these sub-problems simultaneously. The large number of revolutions in step 1 and gravity assists in step 2 and 5 significantly increase the sensitivity of the problem. The dominating gravity sources among these sub-problems are different and it is essential to design them in different coordinates to reduce the difficulty for every step.

Another reason is that the total time of mission is 10 years, while the maximum thrust magnitude is 10 N, so the maximum time of full thrust can be obtained

$$t = \frac{m_{\text{fuel}} I_{\text{sp}} g_0}{T_{\text{max}}}, \tag{6}$$

where T_{max} is the maximum thrust magnitude and m_{fuel} the mass of fuel. Results from eq. (6) show that the total time of full thrust is 51.08 d, which is only 1.4% of the total admissible mission time. If initial costate variables are not guessed properly, the mass of spacecraft will be exhausted rapidly. Numerical singularity occurs when the mass of the spacecraft is near 0 and calculation process has to be terminated, which reduces efficiency seriously.

However, when dividing the mission into 5 sub-problems, the moments for some important events should be chosen carefully to guarantee optimality, such as arriving at the asteroid, leaving the asteroid. They are determined by global searching method. This method is implemented when searching for the best asteroid among all candidates and it is applied to make the result closer to the optimal trajectory.

Experience shows that fuel-optimal problem with long mission time and relatively high thrust can hardly be solved using direct shooting method. However, the problem can be solved if lower thrust magnitude is used. But PMP [34] shows that fuel-optimal control is bang-bang control. That is to say, the optimal thrust is either full or null. Considering two fuel-optimal mission whose difference is only the maximum thrust magnitude, noted as T_1 and T_2. Suppose $T_1 < T_2$ and note that the permission control set for each mission are U_1 and U_2. Because the admissible control set with lower maximum thrust magnitude is a proper subset of the admissible control set with higher maximum thrust magnitude, that is $U_1 \subseteq U_2$, the performance index of the former is definitely worse than the latter.

It's proven that the control law obtained with lower thrust is not optimal, so another approach using direct methods whose control law can ensure that the magnitude of thrust is always the maximum magnitude is proposed. And homotopic approach is also proposed to gradually approximate the maximum thrust magnitude from a lower thrust magnitude.

In step 3 and step 4, the spacecraft has to fly to a selected asteroid and fly back after sampling. The most important thing is to find the proper asteroid among all the candidates. It is obvious that asteroids whose difference in semi-major axis, eccentricity and inclination with the Earth is too large and can be ignored directly and the total number of asteroids to be compared can be reduced.

In preliminary design, the time to leave the Earth, to rendezvous with the asteroid, to leave the asteroid and to use Moon gravity to brake the spacecraft should be determined. And some approximate methods are necessary for quick calculation without great loss of accuracy. For the motion of the spacecraft when flying to the asteroid and flying back to the Earth, two-body model is used to estimate the largest mass that can be collected. The cost of escaping from the Earth-Moon system is chosen to be the same with the cost to accelerate the spacecraft so that it can coast to the Moon's SOI and Moon gravity assist are enough to help the spacecraft to escape from the Earth-Moon system. Lambert problem solver is used to calculate the total velocity increment magnitude needed for the spacecraft to leave the Earth-Moon system to rendezvous with selected asteroid and leave the asteroid to fly back to the Earth-Moon system. After discretizing the launch window, the time cost to fly to the asteroid, the time to leave the asteroid and the time cost to fly back to Moon, grid search is implemented. Two Lambert problems are solved for every node to estimate the mass that can be collected, and the asteroid with the best performance index is selected as the target asteroid.

The initial and final position and velocity are chosen to be the same with those of the Earth. Denote Δv_1 and Δv_2 as the sum of two velocity increments determined from each Lambert problem. And denote m_0 as the mass of the spacecraft when leaving from Earth, M the collected mass and m_{d} the dry mass of spacecraft. The relationship between the col-

lected mass and total sum of velocity increment is

$$\left(m_0 \exp\left(-\frac{\Delta v_1}{I_{sp}g_0}\right) + M\right) \exp\left(-\frac{\Delta v_2}{I_{sp}g_0}\right) = M + m_d. \quad (7)$$

And the largest mass that can be collected is

$$M = \frac{\exp\left(-\dfrac{\Delta v_1 + \Delta v_2}{I_{sp}g_0}\right) m_0 - m_d}{1 - \exp\left(-\dfrac{\Delta v_2}{I_{sp}g_0}\right)}. \quad (8)$$

For every possible transfer, the largest mass that can be collected is estimated through eq. (8). For every asteroid, the possible moments corresponding with the largest sampling mass is selected as the best choice, so does the target asteroid. In this way, the best target asteroid and proper moments can be determined.

In fact, due to Moon gravity assist in step 2, the spacecraft will have certain velocity relative to the Moon and it can be used to reduce the fuel consumption to rendezvous with target asteroid. In step 5, the spacecraft will have a relative velocity with the Moon for gravity assist. So reducing the first and second impulse magnitude of their respective Lambert problems is acceptable. A better approximation is obtained through this way. The result is listed in Table 1.

The classical orbital elements (COE) of the chosen asteroid at epoch 56400 (MJD) are listed in Table 2.

4 Design of all steps

4.1 Design step 1: LEO escape

In this step, thrust is low and many revolutions are required for the spacecraft to get enough velocity to be able to fly to

Table 1 Search result

	Leave earth	Arrive asteroid	Leave asteroid	Arrive earth
Epoch (MJD)	62322	63011	63441	65609

Table 2 Classical orbital elements of target asteroid at epoch 56400 (MJD)

Orbit elements	Values [a]
a (AU)	1.1442
e	0.0968
i (°)	1.695
Ω (°)	120.816
ω (°)	145.382
M (°)	50.255

a) a is the semi-major axis; AU: the astronomical unit (149597870.66 km); e: the eccentricity; i: the inclination; Ω: the ascending node longitude; ω: the argument of perigee and M the mean anomaly

the Moon's SOI. To reduce the fuel consumption, thrust is only applied when the spacecraft is near its perigee. But when the eccentricity of spacecraft's orbit is small, applying thrust in whole arc is also acceptable to reduce the time to escape. Due to the difficulty of the investigated problem, a nominal trajectory is generated as initial guess, and direct optimization methods are used for better convergence performance.

For simplification, thrust direction is assumed to be always the same with the direction of current velocity when generating nominal trajectory. For the first 10 circles, thrust is applied for the whole arc. And for the next 257 circles, thrust is applied only near its perigee and the thrust is applied when the true anomaly is within $[-3\pi/8, 3\pi/8]$. Smaller restrained true anomaly interval may result in better fuel consumption performance but more mission time will be used. A balance between mission time and fuel consumption should be considered.

For effective computation, modified set $(P, e_x, e_y, h_x, h_y, L)$ of Gauss coordinates is used to control the angle of thrust arc. Compared with COE, there is no singularity for circular orbits and zero inclination orbits. The set is defined as follows [35]:

$$\begin{cases} e_x = e\cos(\Omega + \omega), e_y = e\sin(\Omega + \omega), \\ h_x = \tan(i/2)\cos\Omega, h_y = \tan(i/2)\sin\Omega, \\ L = \Omega + \omega + \nu, \end{cases} \quad (9)$$

where P is the semi-latus rectum of the osculating ellipse and ν the true anomaly. The position r and velocity v of the spacecraft in the Cartesian coordinates whose origin is chosen to be the central body are given by

$$r = \frac{P}{CW}\begin{bmatrix} \left(1 + h_x^2 - h_y^2\right)\cos L + 2h_x h_y \sin L \\ \left(1 - h_x^2 + h_y^2\right)\sin L + 2h_x h_y \cos L \\ 2Z \end{bmatrix}, \quad (10)$$

$$v = \frac{1}{C}\sqrt{\frac{\mu_0}{P}}$$
$$\times \begin{bmatrix} 2h_x h_y (e_x + \cos L) - \left(1 + h_x^2 - h_y^2\right)\left(e_y + \sin L\right) \\ \left(1 - h_x^2 + h_y^2\right)(e_x + \cos L) - 2h_x h_y \left(e_y + \sin L\right) \\ 2\left(h_x (e_x + \cos L) + h_y \left(e_y + \sin L\right)\right) \end{bmatrix}, \quad (11)$$

where μ_0 is the gravitational constant of central body and

$$\begin{cases} W = 1 + e_x \cos L + e_y \sin L, \\ Z = h_x \sin L - h_y \cos L, \\ C = 1 + h_x^2 + h_y^2. \end{cases} \quad (12)$$

Denote $x = (P, e_x, e_y, h_x, h_y, L)$ and m the mass of spacecraft. For convenience, the actual thrust vector is defined by

$$\begin{cases} T = uT_{max}\alpha, \\ 0 \leqslant u \leqslant 1. \end{cases} \quad (13)$$

where u is a dimensionless variable representing the thrust magnitude and $\boldsymbol{\alpha}$ the direction of thrust vector. The equations of motion is

$$\dot{\boldsymbol{x}} = \boldsymbol{f}_0(x) + \boldsymbol{f}(x)\frac{uT_{\max}\boldsymbol{\alpha} + \boldsymbol{F}_{\mathrm{per}}}{m},$$
$$\dot{m} = -\frac{uT_{\max}}{I_{\mathrm{sp}}g_0}, \tag{14}$$

where $\boldsymbol{F}_{\mathrm{per}}$ the perturbation and vector field is

$$\boldsymbol{f}_0 = \sqrt{\frac{\mu_0}{P}}\begin{bmatrix} 0 \\ 0 \\ 0 \\ 0 \\ 0 \\ W^2/P \end{bmatrix},$$

$$\boldsymbol{f} = \sqrt{\frac{P}{\mu_0}}$$

$$\times\begin{bmatrix} 0 & 2P/W & 0 \\ \sin L & \cos L + (e_x + \cos L)/W & -Ze_y/W \\ -\cos L & \sin L + (e_y + \sin L)/W & Ze_x/W \\ 0 & 0 & \dfrac{C}{2W}\cos L \\ 0 & 0 & \dfrac{C}{2W}\sin L \\ 0 & 0 & Z/W \end{bmatrix}. \tag{15}$$

Eq. (14) is the derivate of $\boldsymbol{x}$ with respect to time t. Convert it to L for the convenience of determining the start and end of thrust arc, for P, e_x, e_y, h_x, h_y, m

$$\frac{\mathrm{d}x}{\mathrm{d}L} = \frac{\mathrm{d}x}{\mathrm{d}t}\Big/\frac{\mathrm{d}L}{\mathrm{d}t}, \tag{16}$$

and for time t

$$\frac{\mathrm{d}t}{\mathrm{d}L} = 1\Big/\frac{\mathrm{d}L}{\mathrm{d}t}. \tag{17}$$

Combining eq. (14) to eq. (17), derivative of new state parameter $\boldsymbol{x}' = (P, e_x, e_y, h_x, h_y, t, m)$ with respect to L is obtained. And according to the equations of motion described in ECI provided by the organizer, the perturbation of the Moon and Sun is

$$\boldsymbol{F}_{\mathrm{per}} = -\mu_{\mathrm{M}}m\left(\frac{\boldsymbol{r}_{\mathrm{M}}}{r_{\mathrm{M}}^3} + \frac{\boldsymbol{r} - \boldsymbol{r}_{\mathrm{M}}}{\|\boldsymbol{r} - \boldsymbol{r}_{\mathrm{M}}\|^3}\right)$$
$$-\mu_{\mathrm{S}}m\left(\frac{\boldsymbol{r}_{\mathrm{S}}}{r_{\mathrm{S}}^3} + \frac{\boldsymbol{r} - \boldsymbol{r}_{\mathrm{S}}}{\|\boldsymbol{r} - \boldsymbol{r}_{\mathrm{S}}\|^3}\right), \tag{18}$$

$\boldsymbol{r}$ in eq. (18) is usually described in ECI, so is $\boldsymbol{F}_{\mathrm{per}}$, while $\boldsymbol{F}_{\mathrm{per}}$ in eq. (32) is described in local-vertical-local-horizontal (LVLH) frame, in which the x axis points radially away from the center body to spacecraft, the y axis points in the in-track direction with increasing true anomaly, and the z axis points in the cross-track direction. The rotational matrix from LVLH to ECI is

$$\boldsymbol{M} = \begin{bmatrix} \dfrac{\boldsymbol{r}}{\|\boldsymbol{r}\|} & \dfrac{(\boldsymbol{r}\times\boldsymbol{v})\times\boldsymbol{r}}{\|(\boldsymbol{r}\times\boldsymbol{v})\times\boldsymbol{r}\|} & \dfrac{\boldsymbol{r}\times\boldsymbol{v}}{\|\boldsymbol{r}\times\boldsymbol{v}\|} \end{bmatrix}. \tag{19}$$

Perturbation in LVLH is obtained from $\boldsymbol{M}$ and $\boldsymbol{F}_{\mathrm{per}}$ by

$$\boldsymbol{F}'_{\mathrm{per}} = \boldsymbol{M}^{\mathrm{T}}\boldsymbol{F}_{\mathrm{per}}. \tag{20}$$

Now numerical integration of the dynamic equations is conducted. Except for the first full-thrust circles, thrust is applied only when $-3/8\pi \leqslant \nu \leqslant 3/8\pi$, so thrust is applied when $-3/8\pi \leqslant L - (\Omega + \omega) \leqslant 3/8\pi$. To obtain a nominal trajectory, first select the starting time and initial COE of the spacecraft's orbit on LEO, and then integrate in precise dynamic model with the methods mentioned previously. The terminal condition of this step is that the height of the apogee of spacecraft's orbit is equal to the distance between the Earth and Moon so that the spacecraft may coast into Moon's SOI and Moon gravity assist may happen. The termination of numerical integration is implemented using the ode45 subroutine provided by MATLAB.

After integration, the time when the spacecraft coasts to its apogee using simple two-body model is also calculated. Using this arrival time, the phase of the Moon can be determined and the solution is accepted only when the phase of the Moon is near the spacecraft's phase at the arrival time. Otherwise, a new start time should be used. The proper start time is obtained by trial and error, and certain error of constraint violation is acceptable because further local optimization will be used to eliminate it. The nominal trajectory is shown in Figure 1. As Figure 1 shows, the first 10 circles of the nominal trajectory is full-thrust arc and for the next 257 circles, thrust is only imposed when the spacecraft is near its perigee.

After obtaining initial guess, local optimization method is used to not only reduce the fuel cost but also eliminate the violation of constraints of initial guess. Local optimization means that the final solution is not far from initial guess and in order to get better performance index, many initial guesses should be used and the best one is chosen.

The performance index to be minimized is the fuel consumption and the parameters to be optimized are the cumulative longitude (L) of the start and end of coast arc and the direction of thrust for every thrust arc. To parameterize the direction of thrust vector, a polynomial of certain order can be used. In fact, in order to reduce the difficulty of the calculation of analytic partial derivatives of constraint function
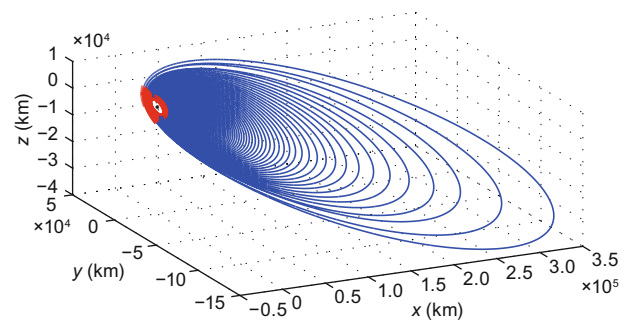

Figure 1 (Color online) Nominal trajectory for step 1.

and cost function with respect to each variable, the order is chosen to be zero, which means the angle between the direction of thrust and velocity vectors is manually chosen to be constant for every single thrust arc.

Because the number of revolutions is large, multiple shooting method is used to reduce the sensitivity of this problem. The variables to be optimized are the states ($\boldsymbol{x}'$) of the start point of thrust arc, cumulative longitude of start and end point, denoted by L_0 and L_f, and two angles to describe the direction of thrust vector, denoted by α and β. For the i-th revolution, integrating with full thrust from L_0^i to L_f^i and from L_f^i to L_0^{i+1} with no thrust, the final state of this revolution $\boldsymbol{x}_t^i$ is obtained and the constraint

$$\boldsymbol{x}_t^i = \boldsymbol{x}_0^{i+1}, \tag{21}$$

where $\boldsymbol{x}_0^{i+1}$ is the state of the start point of $(i+1)$th revolution, should be imposed to ensure the continuity of trajectory. For the last thrust arc, after getting the final state of the end point of thrust arc, another constraint is imposed to ensure Moon gravity assist. With two-body model we can get the state at the apogee of spacecraft's orbit. The position of moon can be calculated following previously mentioned two-body model. The constraint is imposed as:

$$\boldsymbol{r}_{\mathrm{apo}} = \boldsymbol{r}_{\mathrm{moon}}, \tag{22}$$

where $\boldsymbol{r}_{\mathrm{apo}}$ is the position of spacecraft at its perigee, $\boldsymbol{r}_{\mathrm{moon}}$ the position of Moon when spacecraft reaches its perigee.

For multiple shooting method, every revolution is calculated independently, because they are determined only by the parameters of their own. Parallel computation can be implemented, which can significantly accelerate the computing speed.

All the partial derivatives of all constraints and performance index with respect to all variables are computed analytically (not by finite difference). The method is to numerically integrate the variation equations. The calculation of analytic derivatives is difficult and their computation needs a lot of effort and code. But we find that analytic derivatives are crucial to fast execution and robust convergence.

Combining nominal trajectory as initial guess, multiple shooting to reduce sensitivity, parallel computation to accelerate computing speed and analytic partial derivatives, the problem can be solved directly using nonlinear optimization software SNOPT [36]. The local optimal trajectory for the last 257 circles is shown in Figure 2. Because the solution is local optimal, the final trajectory is not far from its initial guess, which also indicates that the initial guess for nominal trajectory is suboptimal. The states at the start and end time of this step is listed in Table 3.

4.2 Design for step 2: Moon gravity assist

In this section, multiple Moon gravity assists with the help of resonant orbit is investigated. After the first Moon gravity
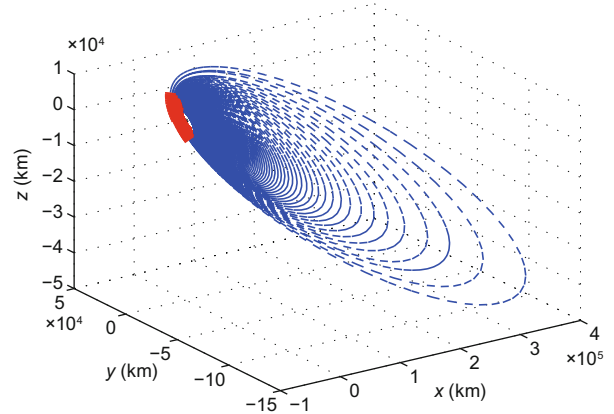
Figure 2   (Color online) Optimal trajectory for step 1.

Table 3   Result for step 1

	Start	End
Epoch	62136	62267
P (km)	6578	22041
e_x	0	-0.880
e_y	0	0.345
h_x	0.175	0.345
h_y	-0.0216	0.153
L	-54.974	1617.7
m (kg)	2000	1769

assist, the spacecraft is guided into an orbit whose period is exactly half of Moon's period. After two revolutions of the spacecraft's orbit, the Moon exactly completes one revolution and another gravity assist can be conducted. As shown in Figure 3, Moon gravity assist is equivalent to an impulse by which the spacecraft's relative speed to the Moon turns an angle. The maximum angle can be calculated through eq. (1).

It can be easily seen from Figure 3 that two gravity assist can greatly change the velocity of the spacecraft.

Equations of motion in precise dynamic model is different from this simplified model and some special methods should be used to optimize trajectories with multiple Moon gravity assist.

4.2.1   Optimal control to nonlinear programming

Because fuel-optimal control is bang-bang control, which means that u can only be 0 or 1, the expected optimal trajectory can be parted into coast arc and full-thrust arc. A way
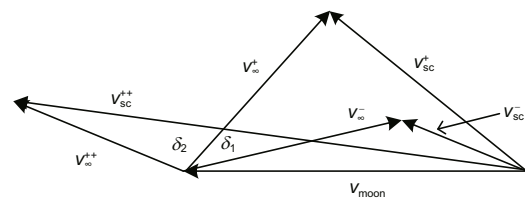
Figure 3   Two moon gravity assists.

to optimize the trajectory is to presuppose the number of full-thrust arcs and use polynomial interpolation to express thrust direction. Described in spherical coordinates, take θ and ϕ as two parameters and the direction of thrust vector can be written as:

$$\alpha = [\cos\theta\cos\phi \quad \cos\theta\sin\phi \quad \sin\theta]^{\mathrm{T}}. \tag{23}$$

With certain order of polynomials to express θ and ϕ, the direction of thrust vector can be calculated. Continuous angle is approximated by limited number of parameters and it is the essence of direct method of trajectory optimization to transform optimal control problem into NLP. However, it is not the coefficients of polynomial, but the value of θ and ϕ on n Chebyshev nodes in the time interval of full-thrust arc are to be optimized. With the value of θ and ϕ on these nodes, a polynomial of $n-1$ order is constructed. If we use coefficients of polynomials to describe the direction, it's difficult to impose constraints on the direction of thrust. Chebyshev nodes in the interval $[a, b]$ are [37]

$$x_k = \frac{1}{2}(a+b) + \frac{1}{2}(b-a)\cos\left(\frac{2k-1}{2n}\pi\right), k = 1, ..., n. \tag{24}$$

To use nonlinear programming to solve optimal trajectory, we can first take m as the number of full-thrust arcs, and n as the order of interpolation polynomials. Parameters to be optimized for one arc are: start and end times, θ and ϕ on every one of $n+1$ Chebyshev nodes. Total number of parameters to be optimized is $m(2n+4)$. Because full thrust is assumed, performance index can be expressed using the sum of the length of every interval

$$\min \sum_{i=1}^{m} \left(t_f^i - t_0^i \right), \tag{25}$$

where t_f^i and t_0^i are start and end times, respectively, of the ith full-thrust arc.

For nonlinear programming problems, constraints should be considered. Constraints for this problem are

(1) Start time of every interval is not more than the end time, that is $t_0^i \leqslant t_f^i$;

(2) Start time of next interval is not less than the end time of current interval, that is $t_f^i \leqslant t_0^{i+1}$;

(3) Constraints on initial and final position and velocity.

For gravity assist problem, special constraints are required. For gravity assist problem in precise dynamic model, due to the strong nonlinearity, the final state of spacecraft is very sensitive to control parameters. Among iteration, it is rather possible that the spacecraft is very close to the Moon, resulting in that dynamic function is extremely nonlinear and numerical problems occur. Calculation has to be terminated. To avoid possible numerical problems by imposing constraints on minimum flyby altitude, the following method is used.

Denote $\boldsymbol{r}_{\mathrm{sc}}, \boldsymbol{v}_{\mathrm{sc}}$ as the position and velocity when spacecraft enters Moon's SOI, and $\boldsymbol{r}_{\mathrm{moon}}, \boldsymbol{v}_{\mathrm{moon}}$ the position and velocity

of Moon at the same time. The spacecraft's relative position and velocity to the Moon are

$$\begin{aligned} \boldsymbol{r}_{\mathrm{rel}} &= \boldsymbol{r}_{\mathrm{sc}} - \boldsymbol{r}_{\mathrm{moon}}, \\ \boldsymbol{v}_{\mathrm{rel}} &= \boldsymbol{v}_{\mathrm{sc}} - \boldsymbol{v}_{\mathrm{moon}}. \end{aligned} \tag{26}$$

The COE of the spacecraft's orbit relative to the Moon is obtained with the relative position and velocity. In general, relative motion is hyperbola and for minimum flyby altitude h_{min}, constraint is

$$a(e-1) \geqslant h_{\mathrm{min}} + R_{\mathrm{moon}}, \tag{27}$$

where h_{min} is the minimum flyby altitude and R_{moon} the radius of moon. Denoting r_{ball} as the radius of Moon's SOI, constraint on the position between spacecraft and the Moon

$$\|\boldsymbol{r}_{\mathrm{rel}}\| = r_{\mathrm{ball}} \tag{28}$$

should also be imposed.

4.2.2 Results and analysis

Based on the method mentioned above, trajectory optimization with multiple gravity assists is transformed into NLP which is solved by SNOPT. The order of polynomial is set to be 2 and three full-thrust arcs, which are assumed that the first two are previous to the first Moon gravity assist and the third is between the first and second Moon gravity assist, are presupposed. The optimal trajectory is shown in Figures 4 and 5. The initial and terminal state of the spacecraft in ECI is shown in Table 4.

It can be found from Figure 4 that in precise dynamic model, the optimal trajectory is not far from preliminarily designed trajectory. After the first Moon gravity assist, the spacecraft coasts in an orbit whose period is about half of the Moon's. The second Moon gravity assist takes place near the first one, not exactly the same because of the influence of both Moon and Sun's gravity. The first flyby altitude is larger than the second one, because the trajectory is not bent as much as the second one, whose flyby altitude is nearly 200 km. And it can be found from Table 4 that 5 kg fuel is used, which accounts for an velocity increment of 97 m/s. In preliminary design, no fuel cost is needed for resonant flybys if the spacecraft moves in a two-body model. In precise dynamic model, because of the gravity of the Moon and Sun, small maneuvers are required to guide the spacecraft into the desired resonant

Table 4 Results for step 2

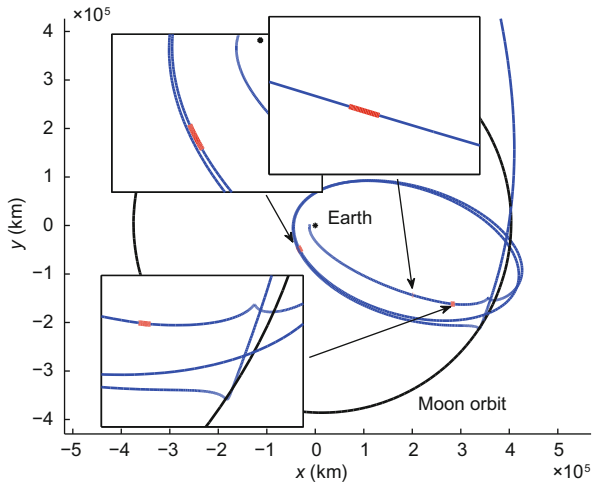|	Start	End
Epoch	62267	62318
x (km)	-1.11×10^4	-1.37×10^4
y (km)	2.48×10^3	1.45×10^6
z (km)	421.6	-3.65×10^5
v_x (km/s)	-2.38	-0.40
v_y (km/s)	-7.51	0.83
v_z (km/s)	-2.438	-0.064
m (kg)	1769	1763

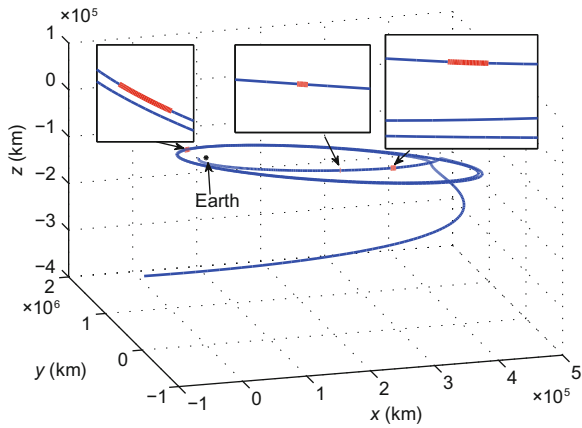**Figure 4**   (Color online) Trajectory projected on *xy* plane with Moon gravity assists.

Figure 5   Spatial trajectory with Moon gravity assists.

orbit. The C_3 at the start time and end time of this step is -1.926 km^2/s^2 and 0.313 km^2/s^2. The time cost is 50.8 d, which is the sum of the time needed to fly to the Moon, the coast time in the resonant orbit, the time to fly out of Earth's SOI.

4.3 Design for step 3: Fly to asteroid

In this step, the spacecraft starts from Earth's SOI and rendezvous with the selected asteroid. The initial state is chosen to be the same with the final state of step 2. The mission time and final state are determined from previous global search. This step can be transformed into a fuel-optimal problem with both initial and final times and states fixed. Long flying time and relatively high thrust magnitude may cause numerical problem as stated before. Here, homotopic methods are used, after solving the same problem with a relatively lower thrust magnitude, the magnitude of thrust is increased gradually until the required magnitude is reached, with former solution as initial guess.

Due to the strong sensitivity of fuel-optimal problem. Homotopic approach is implemented to deal with the difficulty of traditional methods [15,16]. Traditional fuel-optimal problem leads to a bang-bang control law, the shooting function may be discontinuous or non-differentiable at some points [16]. This induces a very narrow convergence domain for nonlinear equations solving methods. Homotopic approach is used by adding a perturbed energy form in the performance index. With the help of this perturbed energy form, the control law of thrust magnitude may become continuous and even derivable. The continuity of the control law is essential to the efficiency and accuracy of numerical integration method, which is used to build TPBVP. And the perturbed energy form can reduce the numerical sensitivity of TPBVP, which can help increase the radius of convergence domain. To help guess the value of initial costate variables, normalization of initial costate variables is implemented and a positive numerical factor λ_0 is added [15]. Note ε be the homotopic parameter with domain [0, 1]. New performance index for fuel-optimal problem is built as:

$$J = \lambda_0 c_2 \int_{t_0}^{t_f} \{ u - \varepsilon \ln [u (1 - u)] \} \, \mathrm{d}t, \qquad (29)$$

where t_0 and t_f denote the initial and final times and are all fixed for this problem and $c_2 = T_{\max}/(I_{\mathrm{sp}} g_0)$.

4.3.1   Optimal control

In this step, the dominating gravity source is the Sun and the problem is considered in HEIRF. All state variables are nondimensionalized using AU as length unit and as for time unit 1 year is normalized to 2π, for better convergence performance.

From eq. (4) the form of the perturbation from Earth and Moon is obtained as:

$$F_{\mathrm{Earth}} = -\mu_{\mathrm{E}} \frac{r_{\mathrm{SC}} - r_{\mathrm{SE}}}{\| r_{\mathrm{SC}} - r_{\mathrm{SE}} \|^3}, \qquad (30)$$

$$F_{\mathrm{Moon}} = -\mu_{\mathrm{M}} \left(\frac{r_{\mathrm{EM}}}{r_{\mathrm{EM}}^3} + \frac{r_{\mathrm{SC}} - r_{\mathrm{SE}} - r_{\mathrm{EM}}}{\| r_{\mathrm{SC}} - r_{\mathrm{SE}} - r_{\mathrm{EM}} \|^3} \right). \qquad (31)$$

In order to decrease the sensitivity of TPBVP, modified set of Gauss coordinates are used as primary variables here instead of components of position and velocity vectors. The new dynamic function is built as:

$$\begin{aligned} \dot{x} &= f_0(x) + f(x) \frac{u T_{\max} \alpha + F_{\mathrm{per}}}{m}, \\ F_{\mathrm{per}} &= F_{\mathrm{Earth}} + F_{\mathrm{Moon}}, \\ \dot{m} &= -\frac{u T_{\max}}{I_{\mathrm{sp}} g_0}. \end{aligned} \qquad (32)$$

First, by introducing Lagrange multiplier $\lambda = (\lambda_x, \lambda_m)$, the Hamiltonian is built as:

$$H = \lambda_x \cdot \dot{x} + \lambda_m \dot{m} + \lambda_0 c_2 \{ u - \varepsilon \ln [u (1 - u)] \}. \qquad (33)$$

Then, the optimal thrust direction and magnitude, which minimize the Hamiltonian, are determined by

$$\alpha = -\frac{f^{\mathrm{T}} \cdot \lambda_x}{\|f^{\mathrm{T}} \cdot \lambda_x\|}, \tag{34}$$

$$u = \frac{2\varepsilon}{\rho + 2\varepsilon + \sqrt{\rho^2 + 4\varepsilon^2}}, \tag{35}$$

where ρ is the switching function (SF) and is determined by

$$\rho = 1 - \frac{I_{\mathrm{sp}} g_0 \|\lambda_v\|}{m\lambda_0} - \frac{\lambda_m}{\lambda_0}. \tag{36}$$

Control law determined in this way is approximating true bang-bang control when ε reduces to 0 gradually and is shown in Figure 6.

As Figure 6 shows, with the reduction of ε from 1 to 0, bang-bang control is approximated gradually. The switching of the sign of SF makes the control law switch between 0 and 1, which agrees with the optimal control without homotopic form [15].

The costate differential equations that termed as Euler-Lagrange equations.

$$\begin{aligned} \dot{\lambda}_x &= -\frac{\partial H}{\partial x}, \\ \dot{\lambda}_m &= -\frac{\partial H}{\partial m}. \end{aligned} \tag{37}$$

Because the final mass is free, the final mass costate variable should be zero

$$\lambda_m(t_f) = 0. \tag{38}$$

The TPBVP consists of a set of equations of the form

$$\Phi = \begin{bmatrix} x(t_f) - x_f \\ \lambda_m(t_f) \\ \lambda_0^2 + \lambda(t_0) \cdot \lambda(t_0) - 1 \end{bmatrix} = 0. \tag{39}$$

To build the TPBVP, initial costate variables and λ_0 are guessed and integration of eqs. (32) and (37) from starting time to ending time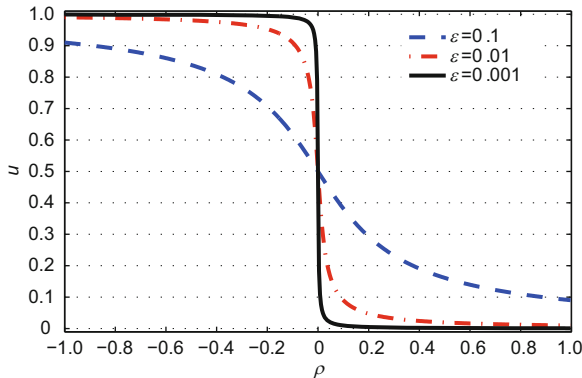 is conducted, with guessing initial costate variables and already known state variables. ε is presupposed initially and is changed with the process of approximating bang-bang control. After integration, all the 8 equations can be built using eq. (39). With 8 equations and 8 variables, single shooting methods such as Powell's or Newton's can be used to solve TPBVP.

4.3.2   Nonlinear equations solving

To solve the shooting function of TPBVP, MinPack-1 [38], a package of FORTRAN subprograms for the numerical solution of systems of nonlinear equations and nonlinear least-squares problems, is used. In MinPack-1, a modification of Powell's hybrid algorithm [39] that is a combination of Newton's method and the method of the gradient is implemented to solve nonlinear equations. The algorithm implemented in MinPack-1 is similar to the solver of MATLAB's fsolve. For the calculation of the Jacobian matrix of this problem, either simply computing by a forward-difference approximation which is implemented by MinPack-1 itself or another rather complicated but more accurate way through numerical integration of the variational equations can be used.

4.3.3   Design for step 3

Design of this step is transformed into a TPBVP with the methods above. Initial maximum magnitude of thrust is chosen to be 0.4 N and ε is chosen to be 0.01. First, increase the maximum magnitude of thrust to 10 N gradually and then decrease ε to 0.0001 gradually, further decrease may cause numerical difficulties but with little improvement in the fuel consumption. The optimal trajectory is obtained as shown in Figures 7 and 8. The history of u is shown in Figure 9. The states at starting and terminating moments of this step is shown in Table 5.

4.4   Design for step 5: Capture

Design for step 5 should be accomplished earlier than step 4 to provide final state and time for step 4. The final state of step 4 is the same with the initial state for step 5 to guarantee the continuity of trajectory. To use Moon gravity assist to
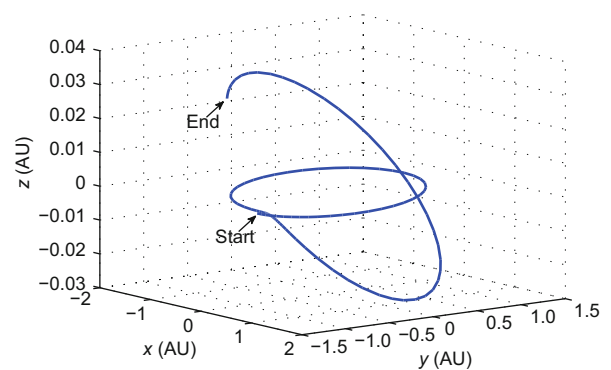
Figure 6   (Color online) Relationship between ρ and u for different ε.

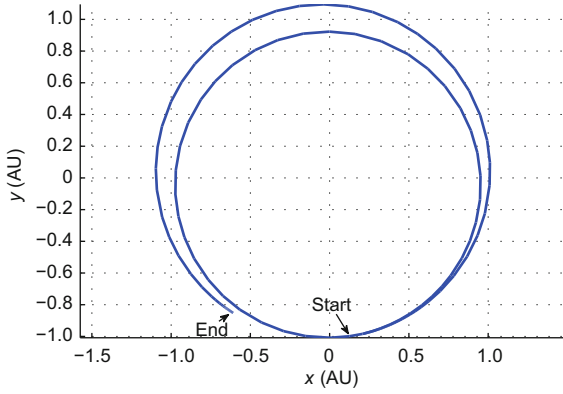**Figure 7**   (Color online) Spatial trajectory to asteroid.

Figure 8 (Color online) Trajectory to asteroid projected on *xy* plane.

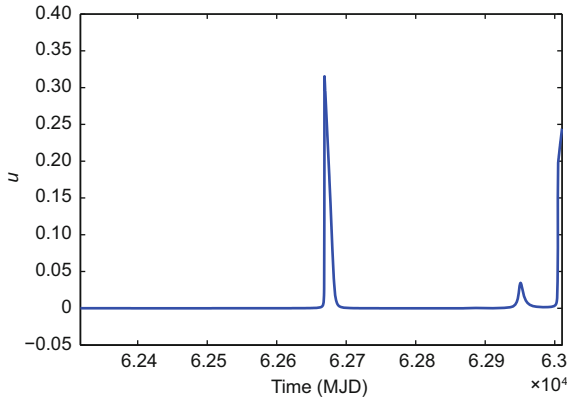**Figure 9** (Color online) Thrust sketches for step 3.

Table 5 Results for step 3

	Start	End
Epoch	62318	63011
P (AU)	0.966	1.13
e_x	0.0181	-6.4×10^{-3}
e_y	0.044	-0.097
h_x	8.28×10^{-4}	-7.58×10^{-3}
h_y	1.34×10^{-3}	0.0127
L	4.93	10.4
m (kg)	1763	1605

reduce the velocity of the spacecraft relative to the Earth, the time and relative position and speed when entering Earth's SOI have to be determined to reduce the fuel consumption for the spacecraft to leave from asteroid to Earth, the final state eq. (2) should also be satisfied.

The position and velocity of spacecraft when entering the Earth's SOI is not easy to determine. By directly solving using optimal control theory for step 4 is almost impossible. The time for every single calculation of step 4 is very long because the narrow convergence domain results in many trials of initial costate variables, which is time consuming. Instead, conic patch leading to Lambert problem is used to approximate the real trajectory.

When the spacecraft enters Earth's SOI, Earth's position r_{earth} and velocity v_{earth} can be obtained through previously mentioned two-body model. The position and velocity of the spacecraft in HEIRF are

$$r_{\text{sc}} = r_{\text{earth}} + r_{\text{rel}},$$
$$v_{\text{sc}} = v_{\text{earth}} + v_{\text{rel}}, \tag{40}$$

where r_{rel} and v_{rel} are spacecraft's position and velocity relative to the Earth. When leaving from the asteroid, the spacecraft's position is the same with asteroid's position and is obtained through previously mentioned two-body model. According to the position when the spacecraft leaves the asteroid and enters the Earth's SOI, Lambert solver is applied to determine the velocity of the spacecraft at corresponding position. Denote v_1 and v_2 as the result of Lambert problem's solution velocities of leaving and arriving, t_m the time when spacecraft enters Moon's SOI and t_f the final time of the mission, t_0 the time when spacecraft enters Earth's SOI. Parameters to be optimized are

$$x = \left[t_0, r_0, v_0, t_m, t_f\right], \tag{41}$$

where r_0 and v_0 are spacecraft's relative position and velocity at t_0. The performance index is

$$\min \left(\|v_1 - v_{\text{ast}}\| + \|v_2 - v_{\text{sc}}\|\right), \tag{42}$$

where v_{ast} is asteroid's velocity vector when spacecraft leaves. Constraints are: the flyby altitude is larger than the minimum, the final condition expressed in eq. (2) should also be satisfied. Nonlinear programming problem is established and SNOPT is used to solve this problem. Trajectory finally obtained is shown in Figure 10. The initial and terminal states of this step are listed in Table 6. The C_3 at the start and end of this step is 1.942 km^2/s^2 and -0.5951 km^2/s^2, respectively.

4.5   Design for step 4: Fly back to the earth

The design of step 4 is very similar to step 2, except that the maximum magnitude of thrust has no need to be changed gradually because the mass of the spacecraft is large after sampling so that even using the maximum magnitude of thrust, the condition that the mass of the spacecraft drops to
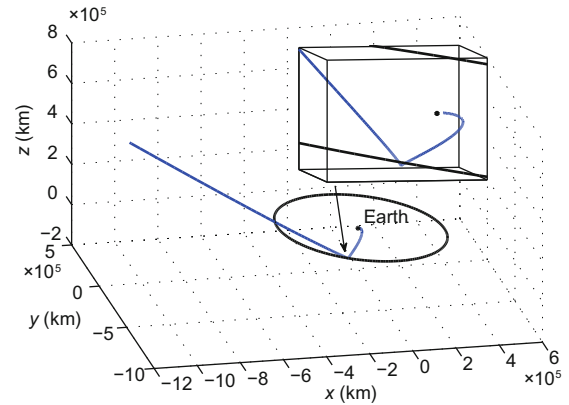

Figure 10 (Color online) Capture trajectory.

Table 6   Results for step 5

	Start	End
Epoch	65607	65618
x (km)	-1.19×10^6	5747.6
y (km)	-5.32×10^5	3199.1
z (km)	7.27×10^5	-30.43
v_x (km/s)	1.28	-7.4
v_y (km/s)	0.15	8.09
v_z (km/s)	-0.897	-0.118

near 0 and numerical difficulty occurs is not very likely to happen.

For the problem discussed here, fuel should be exhausted to ensure as large collected mass as possible. Supposing that m_t is the mass at the final time of this step, M is the collected mass and m_d is the dry mass of spacecraft, it should be satisfied that

$$m_t - M - m_d = 0. \tag{43}$$

With one equality constraint, another costate variable χ is introduced and the product of them is added to generalized index. To maximize the mass of sample is equivalent to maximize the mass when the spacecraft leaves from the asteroid. So the new performance index is

$$J = -\lambda_0 m(t_0) + \lambda_0 c_2 \int_{t_0}^{t_f} \{u - \varepsilon \ln [u(1-u)]\}. \tag{44}$$

With the introduction of one equality constraints, two transversal conditions are introduced.

$$\begin{aligned} \lambda_m(t_0) - \lambda_0 + \chi &= 0, \\ -\lambda_m(t_f) - \chi &= 0, \end{aligned} \tag{45}$$

and χ can be eliminated so that

$$\lambda_m(t_0) - \lambda_m(t_f) - \lambda_0 = 0. \tag{46}$$

There are 9 variables to be solved: costate variables at t_0, λ_0 and the mass when the spacecraft leaves from the asteroid, note as $m(t_0)$. States and costate variables at t_f are obtained through numerical integration from t_0 to t_f. The TPBVP is built as:

$$\Phi = \begin{bmatrix} x(t_f) - x_f \\ \lambda_m(t_0) - \lambda_m(t_f) - \lambda_0 \\ m(t_0) - m(t_f) - m_{fuel} \\ \lambda_0^2 + \lambda(t_0) \cdot \lambda(t_0) - 1 \end{bmatrix} = 0. \tag{47}$$

Using the same method for designing in step 3, start solving with $\varepsilon = 0.01$ and terminate when $\varepsilon = 0.001$ because further reduction of ε is inefficient because of the strong non-linearity and the improvement of $m(t_0)$ is small. The relationship between time and the magnitude of thrust is shown in Figure 11. Bang-bang control is well approximated. The optimal trajectory in HEIRF is shown in Figure 12 and the trajectory in ECI is shown in Figures 13 and 14. The initial
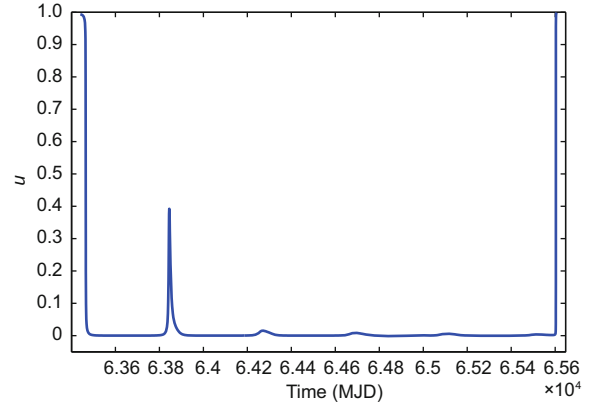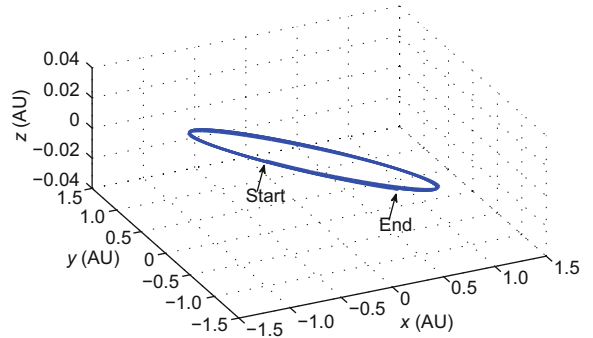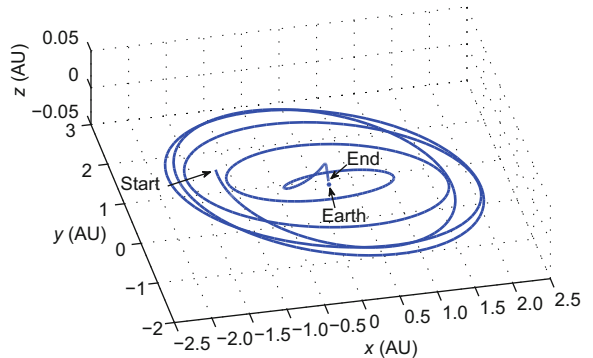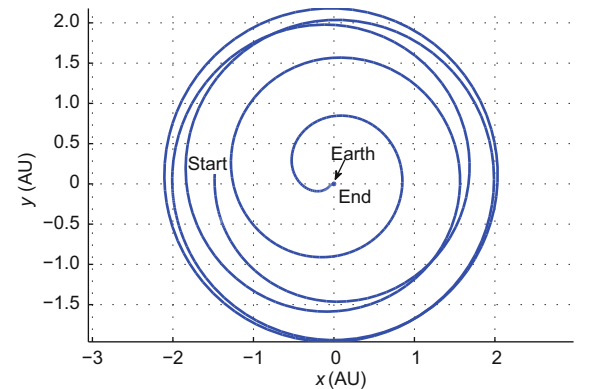

Figure 11   (Color online) Thrust sketches for step 4.

Figure 12   (Color online) Trajectory in HEIRF for step 4.

Figure 13   (Color online) Spatial trajectory in ECI for step 4.

Figure 14   (Color online) Projection of trajectory on *xy* plane in ECI for step 4.

Table 7   Results for step 4

	Start	End
Epoch	63441	65607
P (AU)	1.13	1.09
e_x	-6.4×10^{-3}	0.02392
e_y	-0.0965	-0.0687
h_x	-7.58×10^{-3}	-6.89×10^{-3}
h_y	0.0127	0.0132
L	3.81	36.4
m (kg)	4.62×10^4	4.51×10^4

and terminal state in HEIRF is listed in Table 7. The mass of sample is 44619 kg.

5   Conclusion

This paper presents the method that proposed to solve the problem of NEA sample return mission from LEO. To increase the collected sample mass, practical methods including multiple revolutions and Moon gravity assists are proposed to reduce the fuel consumption to escape from the Earth. Indirect methods are applied to optimize the trajectory to the asteroid, which is selected by global search and the trajectory from asteroid back to the Earth. Multiple Moon gravity assists using resonant orbit is used to increase the velocity when escaping from the Earth and another gravity assist can be taken advantage of to significantly brake the spacecraft when flying back to the Earth.

To reduce the numerical sensitivity of optimizing trajectories with multiple revolutions, multiple shooting methods with parallel computation is used for better convergence performance and computing speed. To avoid the numerical difficulty of indirect method for missions with long period and relatively high thrust, methods such as directly optimizing the moment when the low-thrust engine turns on and off, using polynomials to approximate the direction of thrust and approximating the maximum thrust magnitude gradually are proposed. Preliminary design and further optimization for Moon gravity assists is also investigated. Homotopic methods are used to reduce the sensitivity of indirect methods and the results show that the obtained solution is approximating bang-bang control. And these methods can be easily extended to other missions under more precise dynamic models considering other perturbations.

However, there's still a lot of work that can be done to improve the results. Due to the strong nonlinearity between the mass of sample and the magnitude of the velocity increment that are cost to leave the asteroid and fly back to target destination, the focus should be on this segment. The method of using multiple Moon gravity assist in this segment are to be investigated and it is likely that the mass of sample can increase a lot in this way. Methods to avoid possible numerical difficulty and solve long-time mission with relatively high thrust also need investigation. And the approach to optimize

trajectory with multiple revolutions are also worth researching.

1   Sánchez J P, McInnes C. Available Asteroid Resources in the Earths Neighbourhood. In: Asteroids V B, ed. Berlin, Heidelberg: Springer, 2013. 439–458

2   Yárnoz D G, Sanchez J P, McInnes C. Easily retrievable objects among the NEO population. Celest Mech Dyn Astron, 2013, 116: 367–388

3   Strange N, Landau T M, Lantoine G, et al. Overview of mission design for NASA asteroid redirect robotic mission concept. In: Proceedings of 33rd International Electric Propulsion Conference. Washington D C: The George Washington University, 2013

4   Mingotti G, Sánchez J P, McInnes C. Combined low-thrust propulsion and invariant manifold trajectories to capture NEOs in the Sun-Earth circular restricted three-body problem. Celest Mech Dyn Astron, 2014, 120: 309–336; Mingotti G, Sanchez J P, McInnes C. Low energy, low-thrust capture of near earth objects in the Sun-Earth and Earth-Moon restricted three-body systems. In: Proceedings of SPACE Conferences & Exposition. American Institute of Aeronautics and Astronautics. San Diego, 2014; Hou X Y, Liu L. Double lunar swing-by orbits revisited. Sci China-Phys Mech Astron, 2014, 57: 784–790; Liu X D, Baoyin H X, Ma X R. Dynamics of surface motion on a rotating massive homogeneous body. Sci China-Phys Mech Astron, 2013, 56: 818–829; Wang S, Shang H B, Wu W R. Interplanetary transfers employing invariant manifolds and gravity assist between periodic orbits. Sci China-Phys Mech Astron, 2013, 56: 786–794

5   Xu M, Tan T, Xu S J. Research on the transfers to Halo orbits from the view of invariant manifolds. Sci China-Phys Mech Astron, 2012, 55: 671–683; Chen Y, Baoyin H X, Li J F. Trajectory design for the Moon departure libration point mission in full ephemeris model. Sci China Tech Sci, 2011, 54: 2924–2934; Qi R, Xu S J, Chen T. Control of orientation for spacecraft formations in the vicinity of the Sun-Earth L2 libration point. Sci China-Phys Mech Astron, 2014, 57: 1778–1787; Chen Y, Baoyin H X, Li J F. Design and optimization of a trajectory for Moon departure Near Earth Asteroid exploration. Sci China-Phys Mech Astron, 2011, 54: 748–755

6   Rayman M D, Varghese P, Lehman D H, et al. Results from the deep space 1 technology validation mission. Acta Astron, 2000, 47: 475–487

7   Racca G, Marini A, Stagnaro L, et al. SMART-1 mission description and development status. Planet Space Sci, 2002, 50: 1323–1337

8   Kawaguchi J, Fujiwara A, Uesugi T K. The Ion Engines Cruise Operation And The Earth Swingby Of "Hayabusa" (Muses-C). In: Proceddings of the 55th International Astronotical Congress. Vancouver. 2004

9   Rayman M D, Fraschetti T C, Raymond C A, et al. Coupling of system resource margins through the use of electric propulsion: Implications in preparing for the Dawn mission to Ceres and Vesta. Acta Astron, 2007, 60: 930–938

10   Hargraves C R, Paris S W. Direct trajectory optimization using nonlinear programming and collocation. J Guidance Control Dyn, 1987, 10: 338–342

11   Enright P J, Conway B A. Discrete approximations to optimal trajectories using direct transcription and nonlinear programming. J Guidance Control Dyn, 1992, 15: 994–1002

12   Sims J, Finlayson P, Rinderle E, et al. Implementation of a low- thrust trajectory optimization algorithm for preliminary design. In: Proceed-

ings of AIAA/AAS Astrodynamics Specialist Conference and Exhibit, Guidance, Navigation, and Control and Co-located Conferences. Colorado: American Institute of Aeronautics and Astronautics, 2006

13 Kechichian J A. Optimal low-earth-orbit-geostationary-earth-orbit intermediate acceleration orbit transfer. J Guidance Control Dyn, 1997, 20: 803–811; Guo T D, Jiang F H, Baoyin H X, et al. Fuel optimal low thrust rendezvous with outer planets via gravity assist. Sci China-Phys Mech Astron, 2011, 54: 756–769

14 Ranieri C L, Ocampo C A. Indirect optimization of three-dimensional finite-burning interplanetary transfers including spiral dynamics. J Guidance Control Dyn, 2009, 32: 445–455; Gong S P, Li J F. Fuel consumption for interplanetary missions of solar sailing. Sci China-Phys Mech Astron, 2014, 57: 521–531

15 Jiang F H, Baoyin H X, Li J F. Practical techniques for low-thrust trajectory optimization with homotopic approach. J Guidance Control Dyn, 2012, 35: 245–258; Cai X S, Li J F, Gong S P. Solar sailing trajectory optimization with planetary gravity assist. Sci China-Phys Mech Astron, 2015, 58: 1–11

16 Bertrand R, Epenoy R. New smoothing techniques for solving bang-bang optimal control problemsnumerical results and statistical interpretation. Opt Control Appl Meth, 2002, 23: 171–197; Zhang P, Li J F, Gong S P. Fuel-optimal trajectory design using solar electric propulsion under power constraints and performance degradation. Sci China-Phys Mech Astron, 2014, 57: 1090–1097

17 Kluever C A, Pierson B L. Optimal low-thrust three-dimensional earth-moon trajectories. J Guidance Control Dyn, 1995, 18: 830–837

18 Gao Y, Kluever C A. Low-thrust interplanetary orbit transfers using hybrid trajectory optimization method with multiple shooting. AIAA Paper, 2004, AIAA 2004-5088

19 Hull D G. Conversion of optimal control problems into parameter optimization problems. J Guidance Control Dyn, 1997, 20: 57–60

20 Seywald H. Trajectory optimization based on differential inclusion (Revised). J Guidance Control Dyn, 1994, 17: 480–487

21 Guo T, Jiang F, Li J. Homotopic approach and pseudospectral method applied jointly to low thrust trajectory optimization. Acta Astron, 2012, 71: 38–50

22 Kim Y H, Spencer D B. Optimal spacecraft rendezvous using genetic algorithms. J Spacecraft Rockets, 2002, 39: 859–865

23 Zhu K, Jiang F, Li J, et al. Trajectory optimization of multi-asteroids exploration with low thrust. Jpn Soc Aeron Space Sci Trans, 2009, 52: 47–54

24 Casalino L, Colasurdo G, Pastrone D. Optimal low-thrust escape trajectories using gravity assist. J Guidance Control Dyn, 1999, 22: 637–642

25 Mantia M L, Casalino L. Indirect optimization of low-thrust capture trajectories. J Guidance Control Dyn, 2006, 29: 1011–1014

26 Nah R, Vadali S, Braden E. Fuel-optimal, low-thrust, threedimensional Earth-Mars trajectories. J Guidance Control Dyn, 2001, 24: 1100–1107

27 Mengali G, Quarta A A. Trajectory design with hybrid low-thrust propulsion system. J Guidance Control Dyn, 2007, 30: 419–426

28 Haberkorn T, Martinon P, Gergaud J. Low thrust minimum-fuel orbital transfer: A homotopic approach. J Guidance Control Dyn, 2004, 27: 1046–1060

29 Thevenet J B, Epenoy R. Minimum-fuel deployment for spacecraft formations via optimal control. J Guidance Control Dyn, 2008, 31: 101–113

30 Kawaguchi J, Yamakawa H, Uesugi T, et al. On making use of lunar and solar gravity assists in LUNAR-A, PLANET-B missions. Acta Astron, 1995, 35: 633–642

31 Uphoff C W. The art and science of lunar gravity assist. Adv Astron Sci, 1989, 69: 333–346

32 Macdonald M, McInnes C. Spacecraft planetary capture using gravityassist maneuvers. J Guidance Control Dyn, 2005, 28: 365–369

33 Sims J A. Delta-V gravity-assist trajectory design: Theory and practice. Dissertation for Doctoral Degree. West Lafayette: School of Aeronautics and Astronautics, Purdue University, 1997

34 Pontryagin L S. Mathematical Theory of Optimal Processes. New York: Wiley-Interscience, 1962

35 Gergaud J, Haberkorn T. Orbital transfer: Some links between the lowthrust and the impulse cases. Acta Astron, 2007, 60: 649–657

36 Gill P E, Murray W, Saunders M A. SNOPT: An SQP algorithm for large-scale constrained optimization. SIAM J Opt, 2002, 12: 979–1006

37 Burden R L, Faires J D. Numerical Analysis. 3rd ed. Boston/Mass: Prindle, Weber & Schmidt, 1985

38 Moré J J, Garbow B S, Hillstrom K E. User guide for MINPACK-1. Report. Argonne National Lab. ANL-80-74, 1980

39 Powell M J. A hybrid method for nonlinear equations. Numer Methr Nonlinear Algeb Equat, 1970, 7: 87–114